AIP | Journal of Applied Physics

Key scattering mechanisms limiting the lateral transport in a modulation-doped polar heterojunction

Nguyen Thanh Tien, Dinh Nhu Thao, Pham Thi Bich Thao, and Doan Nhat Quang

Citation: Journal of Applied Physics **119**, 214304 (2016); doi: 10.1063/1.4953030
View online: http://dx.doi.org/10.1063/1.4953030
View Table of Contents: http://scitation.aip.org/content/aip/journal/jap/119/21?ver=pdfcov
Published by the AIP Publishing

Key scattering mechanisms limiting the lateral transport in a modulation-doped polar heterojunction

Nguyen Thanh Tien,[1,a)] Dinh Nhu Thao,[2] Pham Thi Bich Thao,[1] and Doan Nhat Quang[3]
[1]*College of Natural Sciences, Can Tho University, 3-2 Road, Can Tho City, Vietnam*
[2]*Center for Theoretical and Computational Physics, College of Education, Hue University, 34 Le Loi Street, Hue City, Vietnam*
[3]*Institute of Physics, Vietnamese Academy of Science and Technology, 10 Dao Tan Street, Hanoi, Vietnam*

(Received 22 January 2016; accepted 29 April 2016; published online 3 June 2016)

We present a study of the lateral transport of a two-dimensional electron gas (2DEG) in a modulation-doped polar heterojunction (HJ). In contrast to previous studies, we assume that the Coulomb correlation among ionized impurities and among charged dislocations in the HJ is so strong that the 2DEG low-temperature mobility is not limited by impurity and dislocation scattering. The mobility, however, is specified by alloy disorder scattering and combined roughness scattering, which is the total effect induced by both the potential barrier and polarization roughness. The obtained results show that the alloy disorder and combined roughness scattering strongly depend on the alloy content and on the near-interface electron distribution. Our theory is capable of explaining the bell-shaped dependence of the lateral mobility on alloy content observed in AlGaN/GaN and on 2DEG density observed in AlN/GaN, which have not previously been explained. *Published by AIP Publishing*. [http://dx.doi.org/10.1063/1.4953030]

I. INTRODUCTION

Recently, electronic transport and intersubband optical transitions in heterostructures (HSs) based on gallium nitride (GaN), zinc oxide (ZnO), and their compounds have been intensively investigated.[1,2] These properties are characteristic of the quality and performance of electronic and optical devices.[3] These semiconductors possess unique features that are important for fabricating novel electronic and optical devices for high-voltage, high-power, and high-temperature microwave applications.[4]

Electronic transport in HSs is characterized by a high mobility of the two-dimensional electron gas (2DEG) and optical absorption over a narrow spectral linewidth. Both of these properties are determined by electron scatterings that occur in HSs due to phonons, ionized impurities, charged dislocations, interface roughness, and alloy disorder (AD). These properties depend on the parameters of the HS, such as temperature, 2DEG density, and alloy content. By analyzing the related experimental data, one can realize the key scattering mechanisms that limit the lateral transport and optical intersubband transitions to determine approaches to reduce their adverse actions.

Key scattering mechanisms are of paramount importance and are specified by the used regime of parameters. At very low temperature, phonon scattering is negligible. Modulation doping is a technique for reducing impurity scattering.[5] Moreover, due to ionic correlation caused by Coulomb repulsion among ionized impurities during their diffusion in samples subject to thermal treatment (annealing), their distribution becomes more microscopically homogeneous; thus, the scattering from remote impurities can be further reduced (by more than one order of magnitude), and their effect is not strong enough to limit the 2DEG mobility.[6,7]

The scattering rate from charged dislocations was found[8–11] to be proportional to the square of the fraction of filled traps introduced by dislocations, f ($0.1 \leq f \leq 0.5$). In the literature,[12–15] this scattering was exaggerated with the choice $f = 1$. A comparison with mobility data obtained for AlGaN/GaN at rather high 2DEG densities ($n_s \gtrsim 10^{12}$ cm^{-2}) led to the hypothesis[1,16] that the dislocation scattering even with $f = 1$ is not strong enough to limit 2DEG mobilities at present and that there must be stronger scattering mechanisms in operation. This is further supported by the fact that each dislocation has a lower filling fraction due to correlations among them.[13]

It is well known that[1,2] polarization is an important property of nitride- and oxide-based HSs. These HSs possess a very high (areal) density of polarization charges bound to their interfaces ($\sigma \sim 10^{13}$ cm^{-2}). We have recently shown[17] that these charges have a three-fold role similar to the ionized impurities. The polarization charges on a rough interface are a carrier supply source, a confining source, and a scattering mechanism for HSs. We showed that the geometric roughness of an interface between material layers forming a polar HS may cause two physical phenomena: barrier roughness (BR) and polarization roughness (PR). The roughness of an interface produces simultaneous fluctuations in the position of the potential barrier and in the position of the interface polarization charges. The fluctuations of both types act in combination on the lateral transport as an *ad hoc* mechanism referred to as combined roughness (CR) scattering, while the BR in the literature is simply referred to as interface roughness scattering. Therefore, in contrast to previous studies,[13–15,18] we assume that the low-temperature mobility of a high-density 2DEG in modulation-doped polar

a)Electronic mail: nttien@ctu.edu.vn. Fax: +84 710 3832062.

HSs is limited not by scattering from remote ionized impurities and charged dislocations but rather by scattering from alloy disorder (AD) and combined roughness.

The 2DEG mobility in polar HSs, e.g., AlGaN/GaN, was intensively studied both experimentally[19–22] and theoretically.[12–15,18,23,24] The measurement detected a pronounced peak in the 2DEG mobility dependence on the Al content of the AlGaN alloy[19,20] and the 2DEG density.[22] However, no theoretical analysis of its bell shape has yet been conducted. Moreover, there were some drawbacks with the previous calculations.[12–15,18,23,24] In those studies, the interface polarization charges were taken into account only as a carrier supply source; these charges were often omitted as a confining source and were always omitted as a scattering mechanism. In addition, the confinement effect was calculated within the infinite barrier,[13–15] which is a good approximation only for describing bulk phenomena, such as scattering from phonons, impurities, and dislocations.

Thus, the aim of this work is to present a theory for the 2DEG lateral transport in modulation-doped polar HSs to explain the bell shape of the 2DEG mobility dependence on the alloy content and on the 2DEG density. Moreover, our theory may also explain the influence of the AlN layer on the 2DEG mobility in the undoped AlN/GaN heterojunction. In this way, the effects of all confining sources and all scattering mechanisms are properly taken into account. The remainder of this paper is organized as follows. In Sec. II, we formulate the basic equations for calculating the low-temperature transport lifetime in heterojunctions (HJs). In Sec. III, we present the autocorrelation functions (ACFs) for two scattering mechanisms (AD and CR). Section IV presents numerical results for the 2DEG mobility dependence on experimental conditions, such as alloy content, 2DEG density, and doping profile. Finally, a summary is presented in Sec. V.

II. LOW-TEMPERATURE TRANSPORT LIFETIME

In this section, we address the low-temperature lateral transport of the 2DEG in a modulation-doped polar HJ. For this purpose, we have formulated the basic equations that are required for calculating the transport lifetime.

As is known,[3] electrons that move in-plane are scattered by various disorder sources, which are normally characterized by some random fields. Scattering by a Gaussian random field is specified by its autocorrelation function in wave vector space, $\langle|U(\mathbf{q})|^2\rangle$. Here, $U(\mathbf{q})$ is a 2D Fourier transform of the unscreened potential weighted with the lowest subband wave function

$$U(\mathbf{q}) = \int_{-\infty}^{+\infty} dz\, |\zeta(z)|^2 U(\mathbf{q}, z). \tag{1}$$

At rather high 2DEG densities ($n_s \gtrsim 10^{12}\,\mathrm{cm}^{-2}$), the multiple scattering effects are negligibly small,[25] and thus, we may adopt the linear transport theory as a good approximation. The inverse transport lifetimes at low temperature are then represented in terms of the ACF for each disorder as follows:[26,27]

$$\frac{1}{\tau} = \frac{1}{2\pi\hbar E_F} \int_0^{2k_F} dq \frac{q^2}{\left(4k_F^2 - q^2\right)^{1/2}} \frac{\langle|U(\mathbf{q})|^2\rangle}{\varepsilon^2(q)}. \tag{2}$$

Here, $\mathbf{q}$ denotes the momentum transfer vector by a scattering event in the interface plane, $q = |\mathbf{q}| = 2k_F \sin(\vartheta/2)$, with ϑ as the scattering angle. The Fermi wave number is fixed by the electron sheet density: $k_F = \sqrt{2\pi n_s}$ and $E_F = \hbar^2 k_F^2/2m^*$, with m^* as the in-plane effective mass of the GaN electron.

The dielectric function $\varepsilon(q)$ entering Eq. (2) allows for the screening of scattering potentials by the 2DEG. As usual, this is evaluated within the random phase approximation[3,28]

$$\varepsilon(q) = 1 + \frac{q_s}{q} F_S(q/k)\,[1 - G(q/k)], \quad \text{for } q \le 2k_F, \tag{3}$$

with $q_s = 2m^* e^2/\varepsilon_a \hbar^2$ as the inverse 2D Thomas-Fermi screening length, where ε_a is the average dielectric constant of two material layers.

The screening form factor $F_S(t)$ depends on the electron distribution confined along the growth direction. For a triangular quantum well, this is derived as[28]

$$\begin{aligned} F_S(t) = {} & \frac{A^4 a}{t+a} + 2A^2B^2 a \frac{2 + 2c(t+1) + c^2(t+1)^2}{(t+a)(t+1)^3} \\ & + \frac{B^4}{2(t+1)^3}\left[2\left(c^4 + 4c^3 + 8c^2 + 8c + 4\right)\right. \\ & + t\left(4c^4 + 12c^3 + 18c^2 + 18c + 9\right) \\ & \left. + t^2\left(2c^4 + 4c^3 + 6c^2 + 6c + 3\right)\right]. \end{aligned} \tag{4}$$

Here, we introduced dimensionless wave numbers in the interface plane (t) and the barrier (a) by definition

$$t = q/k, \quad a = \kappa/k. \tag{5}$$

The quantum confinement of electrons are taken into account within the finite potential barrier model and bent band determined by all confinements.[29,30]

The local field corrections are due to the many-body exchange effect in the in-plane, given by[31]

$$G(t) = \frac{t}{2\left(t^2 + t_F^2\right)^{1/2}}, \quad \text{with } t_F = k_F/k. \tag{6}$$

As shown in Sec. I, because of the strong Coulomb correlation among ionized impurities and among charged dislocations, the electrons in a modulation-doped polar HJ are expected to essentially experience the following scattering mechanisms: (i) alloy disorder (AD) and (ii) combined roughness (CR). The overall transport lifetime is determined by the mechanisms due to individual disorders in accordance with Matthiessen's rule

$$\frac{1}{\tau_{tot}} = \frac{1}{\tau_{AD}} + \frac{1}{\tau_{CR}}. \tag{7}$$

At low temperature, the mobility is generally determined via this transport lifetime τ by

$$\mu = e\tau/m^*. \tag{8}$$

III. AUTO CORRELATION FUNCTIONS FOR KEY SCATTERING MECHANISMS IN POLAR HETEROSTRUCTURES

A. Alloy disorder

In the calculation of the transport lifetime using Eq. (2), the ACFs in wave vector space, $\langle|U(\mathbf{q})|^2\rangle$, play a vital role. Thus, we must specify them for identifying the key scattering mechanisms in a modulation-doped polar HJ.

The alloy is located in the barrier layer. Because the alloy disorder is a short (zero)-range interaction,[32] this affects the tail of the z-axis electron distribution in the barrier only from $-L_a$, where L_a is the distance from the layer that is composed of both host and alloy atoms and that is the closest to the interface ($L_a \sim 3.3$ Å).[33–35] With the wave function in a triangular well within the finite potential barrier model,[30] the ACF for AD scattering was derived as[17,29,32]

$$\langle|U_{AD}(\mathbf{q})|^2\rangle = x(1-x)u_{al}^2\Omega_0 f_{AD}, \tag{9}$$

where f_{AD} is the form factor for AD scattering given in terms of the barrier wave number κ by

$$f_{AD} = \frac{A^4\kappa}{2}[e^{-2\kappa L_a} - e^{-2\kappa L_b}]. \tag{10}$$

In Eq. (9), x is the Al content in the barrier, L_b is the barrier thickness, u_{al} is the alloy potential, and Ω_0 is the volume occupied by one atom. The alloy potential is an adjustable parameter for fitting to experimental data[36] and is generally assumed[32] to be close to the conduction band offset between the two binaries forming the alloy: $u_{al} \sim \Delta E_c(1)$. The atomic volume Ω_0 is related to the volume of the alloy unit cell Ω_c. For hexagonal wurtzite crystals, there are 4 atoms per unit cell:[37] $\Omega_0 = \Omega_c/4$, where $\Omega_c = (\sqrt{3}/2)a^2(x)c(x)$ with $a(x)$ and $c(x)$ as the lattice constants of the alloy.

Note that for a large barrier thickness L_b, the second term in Eq. (10) is negligible. Thus, AD scattering is primarily determined by the first term proportional to $\zeta^4(z=-L_a)$, i.e., by the near-interface value of the electron wave function.

B. Combined roughness

As stated above, CR scattering is the total effect from two roughness-induced scatterings: barrier roughness and polarization roughness. The ACF for this effect reads as[17]

$$\langle|U_{CR}(\mathbf{q})|^2\rangle = |F_{CR}(t)|^2\langle|\Delta_{\mathbf{q}}|^2\rangle, \tag{11}$$

where the relevant form factor is given by the sum

$$F_{CR}(t) = F_{BR} + F_{PR}(t), \tag{12}$$

where F_{BR} is the form factor for scattering from barrier roughness and $F_{PR}(t)$ is from polarization roughness.

We are now concerned with the form factor for BR scattering. This is fixed by the local value of the electron wave function at the interface plane ($z=0$) as follows:[3]

$$F_{BR}^{loc} = V_0|\zeta(0)|^2. \tag{13}$$

For a sufficiently high potential barrier, one may replace the wave function by its derivative such that[38]

$$F_{BR}^{loc} \approx \frac{\hbar^2}{2m_z}|\zeta'(0)|^2. \tag{14}$$

Thus, BR scattering is determined by the electron distribution at the interface plane.

As previously reported,[38,39] relative errors caused by using the value of approximate wave functions at $z=0$ may be large in the calculation of BR (and CR) scattering because this local value for a bound state is typically very small [$\zeta(0) \sim 0$]. To avoid serious errors associated with the use of approximate (variational) wave functions in the case where BR scattering is a key scattering mechanism, we should express the BR form factor not in terms of this local value but rather in terms of a non-local quantity, such as the integral for the average of the electrostatic confining forces. Consequently, we have[6,7]

$$F_{BR}^{nloc} = \langle V_\sigma'\rangle + \langle V_I'\rangle + \langle V_s'\rangle, \tag{15}$$

where $V' = \partial V(z)/\partial z$. Note that the BR form factors given by Eqs. (13) and (15) are equal if $\zeta(z)$ is an exact wave function.

With the use of the ground-state wave function of a triangular quantum well, even within the finite potential barrier model,[30] the calculation of the average forces in Eq. (15) is straightforward. These are listed below.

For the polarization charges of density σ,

$$\langle V_\sigma'\rangle = \frac{4\pi e^2}{\varepsilon_a}\frac{\sigma}{2e}(1-2A^2). \tag{16}$$

For the remote ionized impurities of sheet density n_I,

$$\langle V_I'\rangle = \frac{4\pi e^2 n_I}{\varepsilon_a}\left\{1 - A^2 - \frac{A^2}{d-s}[\chi_1(d) - \chi_1(s) - d\chi_0(d) + s\chi_0(s)]\right\}. \tag{17}$$

For the 2DEG distribution of sheet density n_s,

$$\langle V_s'\rangle = -\frac{4\pi e^2 n_s}{\varepsilon_a}\left[1 - A^2 + \frac{A^4}{2} - \frac{B^4}{2}\times(c^4+4c^3+8c^2+8c+4)\right]. \tag{18}$$

Next, the form factor for PR scattering was derived as[17]

$$F_{PR}(t) = \frac{2\pi e\sigma}{\varepsilon_a}\left\{\frac{B^2}{r_\varepsilon}\left[\frac{2}{(t+1)^3} + \frac{2c}{(t+1)^2} + \frac{c^2}{t+1}\right] - A^2\frac{a}{t+a}\right\}. \tag{19}$$

The PR scattering is anisotropic, occurring essentially forward ($\vartheta \sim 0$), whereas the BR one is isotropic.

IV. THE 2DEG MOBILITY IN POLAR HETEROJUNCTIONS

A. Partial mobilities limited by AD and CR scattering

In previous studies of lateral 2DEG transport in HJs,[14,15,21,24] the calculations were performed within the

infinite barrier model based on the standard Fang-Howard wave function.[3,40] This model essentially simplified the mathematics of the transport theory and was a good approximation for scattering mechanisms that are insensitive to the near-interface wave function, such as phonons, ionized impurities, and charged dislocations. In the case under investigation, the key scattering mechanisms (AD and CR) are, in contrast, quite sensitive. Thus, we examined the confinement effect within the finite barrier model based on the modified Fang-Howard wave function[29] and the bent banding effect by all confining sources.[30] As an example, we used the modulation-doped polar AlGaN/GaN HJ with a fixed finite barrier, being equal to the conduction band offset for $x = 0.3$: $V_0 = 0.45$ eV. We determined that the electron distribution in the finite barrier and infinite barrier models are changed in opposite directions by varying the donor bulk density and the polarization charge density.[30] Here, we consider the dependence of the mobilities of 2DEGs in polar HJs on various parameters, such as the densities of interface polarization charges and doping profile. To provide a representative illustration, we adopt the simplifying assumption that one of the parameters is varied while the others are fixed. However, to explain the experimental data in Subsection IV B, all the relations among them are taken into account.

We calculate the partial mobilities limited by the AD scattering and the CR scattering using Eqs. (2), (8), (9) and (11). First, in Fig. 1, the electron mobilities in the modulation-doped polar AlGaN/GaN HJs are plotted versus polarization charge density σ/e for a 2DEG density of $n_s = 5 \times 10^{12}\,\mathrm{cm}^{-2}$. The modulation doping is with a density of $N_I = 5 \times 10^{18}\ \mathrm{cm}^{-3}$, a thickness of doping $L_d = 150$ Å, and spacer $L_s = 70$ Å. The interface profile of HJs is fixed with a roughness amplitude of $\Delta = 3$ Å and a correlation length of $\Lambda = 70$ Å.

Next, in Fig. 2, we examine the dependence of these partial mobilities on the modulation doping profile (density N_I) for an Al content in the AlGaN alloy of $x = 0.3$ and a 2DEG density of $n_s = 5 \times 10^{12}\ \mathrm{cm}^{-2}$. These are plotted for a doping thickness of $L_d = 150$ Å and a spacer thickness of $L_s = 70$ Å. The interface profile of HJs is fixed with a roughness amplitude of $\Delta = 3$ Å and a correlation length of $\Lambda = 70$ Å.

From the obtained lines, we may draw the following conclusions.

(i) Within the infinite-barrier model, the AD scattering is excluded because the 2DEG is spatially separated from the alloy disorder. The CR mobility is decreased with increasing sheet densities of polarization charges because the 2DEG is shifted toward the interface and its peak is increased. In this model, the role of the modulation doping is not important. It has been considered that the modulation doping does not affect the electron mobility because it moves the electronic distribution region far away.

(ii) In contrast, within the finite-barrier model, both the AD and CR scatterings significantly affect the electron mobilities. The CR scattering increases with increasing polarization charge density σ/e, and this scattering slightly increases as the donor bulk density N_I increases. In addition, the AD scattering decreases with increasing polarization charge density, and this scattering increases as the donor bulk density

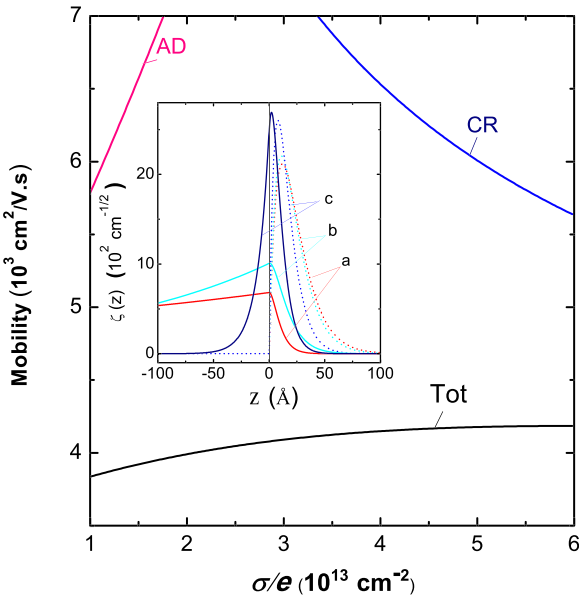

FIG. 1. Partial mobilities in AlGaN/GaN modulation-doped HJ limited by alloy disorder (AD), combined roughness (CR), and overall (Tot) scatterings vs. polarization charge density σ/e. The interface profile of HJs is fixed with $\Delta = 3$ Å and $\Lambda = 70$ Å. The inset shows the wave function in an AlGaN/GaN HJ for a 2DEG density of $n_s = 5 \times 10^{12}\ \mathrm{cm}^{-2}$, a modulation doping of donor bulk density of $N_I = 5 \times 10^{18}\ \mathrm{cm}^{-3}$, a doping thickness of $L_d = 150$ Å, a spacer of $L_s = 70$ Å, and various polarization-charge densities $\sigma/e = 5 \times 10^{12}$, 10^{13}, and $5 \times 10^{13}\ \mathrm{cm}^{-2}$, labeled a, b, and c, respectively.[30]

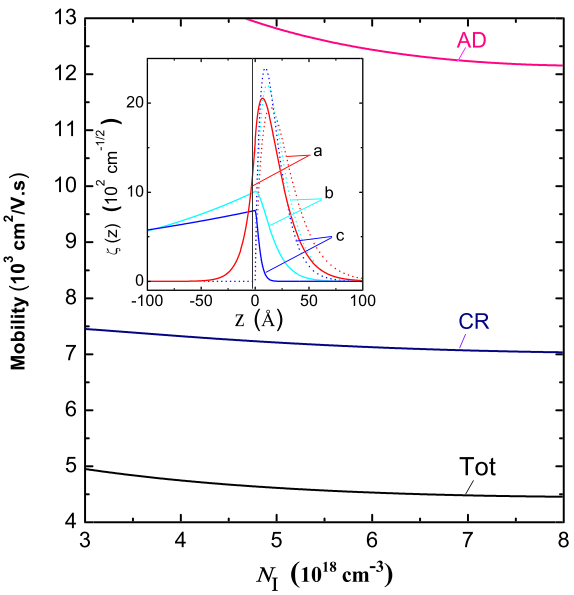

FIG. 2. Partial mobilities in modulation-doped AlGaN/GaN HJs with an Al content in the alloy of $x = 0.3$, a 2DEG density of $n_s = 5 \times 10^{12}\ \mathrm{cm}^{-2}$, a doping thickness of $L_d = 150$ Å and a spacer thickness of $L_s = 70$ Å limited by alloy disorder (AD), combined roughness (CR), and overall (Tot) scatterings vs doped bulk density N_I. The interface profile of HJs is $\Delta = 3$ Å and $\Lambda = 70$ Å. The inset shows the wave functions in an AlGaN/GaN HS for a 2DEG density of $n_s = 5 \times 10^{12}\ \mathrm{cm}^{-2}$, a modulation doping with a doping thickness of $L_d = 150$ Å, a spacer thickness of $L_s = 70$ Å, and various donor bulk densities of $N_I = 10^{18}, 5 \times 10^{18}$, and $10^{19}\,\mathrm{cm}^{-3}$ labeled a, b, and c, respectively.[30]

increases. This is associated with the electron distribution, as shown in the inset.

(iii) Moreover, Figs. 1 and 2 show that both of the scattering mechanisms (AD and CR) are important. Which scattering is exceeding, AD scattering or CR scattering? The answer to this question depends on the properties of the profiles of the system (doping, rough interface, and polarization charge density).

B. Total mobility: Theory versus experiment

As shown above, low-temperature lateral 2DEG transport in a polar HS is limited by AD and CR scatterings that are very sensitive to the near-interface 2DEG distribution. By considering the influence of all confining sources on the electron wave function (viz., the potential barrier and the electrostatic sources: interface polarization charges, ionized donors, and 2DEG), we have examined the role of the interface polarization charges and the bulk donor density effect on partial mobilities. However, the multitude of the relevant parameters can make the analysis of the influence of an individual confining source rather difficult. For instance, a change in the Al content in the alloy implies a variation in many quantities, such as the barrier height $V_0(x)$, polarization charge density $\sigma(x)$,[33,41,42] 2DEG density $n_s(x)$,[1,33] and potentially roughness profile: $\Delta(x)$, $\Lambda(x)$.[20,21]

To confirm the validity of our model, we apply our theory to explain the recent experimental data regarding the dependence of low-temperature 2DEG mobility on the parameters of interest: alloy content and 2DEG density. In Fig. 3, we present the partial mobilities in the AlGaN/GaN HJ versus Al content in the alloy x for a modulation doping of $N_I = 4 \times 10^{18}$ cm^{-3}, $L_d = 150$ Å, and $L_s = 70$ Å. The barrier height $V_0(x)$, polarization charge density $\sigma(x)/e$, and 2DEG density $n_s(x)$ vary with x. The interface profile (Δ, Λ) also varies with x.[20] The solid lines and circles refer to the calculated mobilities within finite confinement and the measured mobilities[20] at 77 K, respectively.

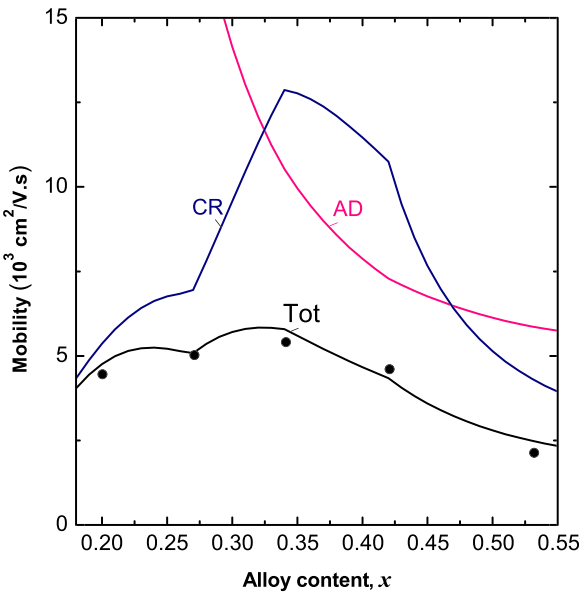

FIG. 3. Partial mobilities in an AlGaN/GaN HJ under a modulation doping of $N_I = 4 \times 10^{18}$ cm^{-3}, $L_d = 150$ Å, and $L_s = 70$ Å vs. aluminum content x. The barrier height $V_0(x)$, sheet polarization charge density $\sigma(x)$, and 2DEG density $n_s(x)$ vary with x. The interface profile (Δ, Λ) perhaps varies with x.[20] The solid lines refer to the calculated mobilities within finite confinement, and the 77 K experimental mobility data[20] are marked by circles.

Fig. 3 reveals that both alloy disorder and polarization surface roughness scatterings are important in limiting the measured mobility. The former is responsible for the increasing mobility at small alloy content, whereas the latter displays a bell-shaped curve. The total mobility strongly depends on the polarization surface roughness scattering.

Finally, in Fig. 4, we present the calculated mobilities versus 2DEG density n_s for the undoped HJs produced from $Al_xGa_{1-x}N$/GaN of $x = 0.27$ and AlN/GaN ($x = 1$). The solid lines refer to the mobilities calculated for $Al_{0.27}Ga_{0.73}N$/GaN (AD, CR, and total) and AlN/GaN (total = CR). The interface profiles ($\Delta = 3$ Å, $\Lambda = 70$ Å) and ($\Delta = 6$ Å, $\Lambda = 120$ Å) are applied for the $Al_{0.27}Ga_{0.73}N$/GaN structure and the AlN/GaN one, respectively. We also show the mobilities measured in the $Al_{0.27}Ga_{0.73}N$/GaN HJ and AlN/GaN HJ at 20 K by Smorchkova *et al.*[43]

From the obtained lines, we may draw the following conclusions.

(i) The 2DEG channel lies very close to the interface, and thus, it can be very sensitive to any physical processes that occur at the interface of the sample.

(ii) With CR scattering, we are able to well reproduce the data regarding the density dependence of 2DEG mobility in the HJs. The agreement is quantitative for the HJs of a fixed Al composition ($x = 0.7$ and $x = 1$), while the interface profile can be chosen as the fitting parameters.

(iii) With the undoped polar AlN/GaN heterojunction, the AD scattering is so small as to be negligible due to

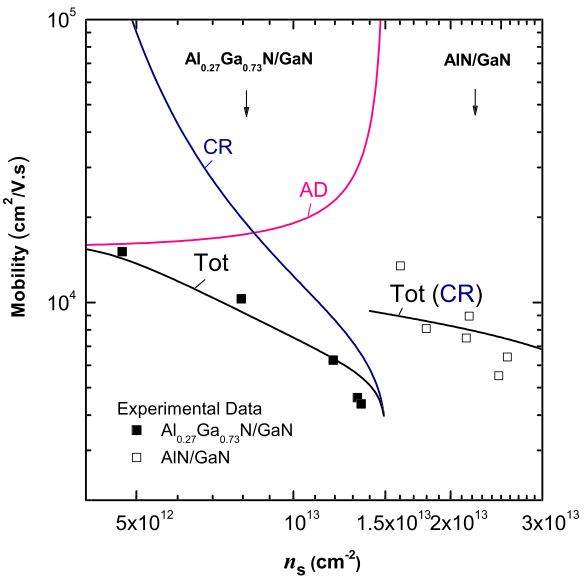

FIG. 4. Influence of the AlN layer on the 2DEG mobility in the undoped HJs. The solid and dashed lines refer to the mobilities calculated within the finite barrier model for the 2DEG in AlGaN/GaN ($x = 0.27$) and AlN/GaN ($x = 1$), respectively. The solid and empty squares refer to the mobilities measured at 20 K in the former and latter HJs, respectively.[43]

the high barrier potential, and hence, the CR scattering becomes important. We observe that the changing trend of mobility vs. n_s is similar to the $Al_xGa_{1-x}N$/GaN HJ case. The only difference is the magnitude of the mobility.

V. SUMMARY

To summarize, in this work, we have demonstrated that alloy disorder and combined roughness scatterings depend strongly on the alloy content and the near-interface electron distribution. These two scattering mechanisms have important roles in the lateral transport of a two-dimensional electron gas in a modulation-doped polar heterojunction.

By taking all effects from polarization charges (carrier supply source, confining source, and scattering mechanism), the finite confinement effect and the screening effect into account, our theory provided a good quantitative explanation of the different evolution of 2DEG mobility versus carrier density and alloy content in modulation-doped polar heterojunctions. Our theory is also capable of explaining the influence of the AlN layer on the 2DEG mobility in the polar AlN/GaN HJs.

We determined that the infinite potential barrier model is applicable, as a good approximation, only to scatterings that are insensitive to the near-interface 2DEG distribution, e.g., ionized impurities and phonons. For scatterings that are sensitive to this distribution, e.g., alloy disorder and roughness-related scatterings, the finite potential barrier model must be applied. To determine the optimal HJ structures, we need to include many different constituents simultaneously.

ACKNOWLEDGMENTS

This work was supported by the Vietnamese National Foundation for Science and Technology Development (NAFOSTED 103.02-2012.04) and by the Vietnam Ministry of Education and Training. Part of this work was conducted during the stay of one of the authors (N. T. Tien) at Uppsala University in the framework of the Erasmus Mundus Scholarship.

[1]D. Jena, in *Polarization Effects in Semiconductors*: From Ab Initio Theory to Device Applications, edited by C. Wood and D. Jena (Springer, New York, 2008), p. 161.
[2]*Oxide and Nitride Semiconductors*, edited by T. Yao and S.-K. Hong (Springer, Berlin-Heidelberg, 2009).
[3]T. Ando, A. B. Fowler, and F. Stern, Rev. Mod. Phys. **54**, 437 (1982).
[4]O. Manasreh, *Introduction to Nanomaterials and Devices* (John Wiley & Sons, 2012).
[5]R. Dingle, H. L. Störmer, A. C. Gossard, and W. Wiegmann, Appl. Phys. Lett. **33**, 665 (1978).
[6]D. N. Quang, V. N. Tuoc, N. H. Tung, N. V. Minh, and P. N. Phong, Phys. Rev. B **72**, 245303 (2005).
[7]D. N. Quang, L. Tuan, and N. T. Tien, Phys. Rev. B **77**, 125326 (2008).
[8]N. G. Weimann, L. F. Eastman, D. Doppalapudi, H. M. Ng, and T. D. Moustakas, J. Appl. Phys. **83**, 3656 (1998).
[9]H. M. Ng, D. Doppalapudi, T. D. Moustakas, N. G. Weimann, and L. F. Eastman, Appl. Phys. Lett. **73**, 821 (1998).
[10]K. Leung, A. F. Wright, and E. B. Stechel, Appl. Phys. Lett. **74**, 2495 (1999).
[11]D. M. Schaadt, E. J. Miller, E. T. Yu, and J. M. Redwing, Appl. Phys. Lett. **78**, 88 (2001).
[12]D. Jena, A. C. Gossard, and U. K. Mishra, Appl. Phys. Lett. **76**, 1707 (2000).
[13]M. N. Gurusinghe and T. G. Andersson, Phys. Rev. B **67**, 235208 (2003).
[14]D. Zanato, S. Gokden, N. Balkan, B. K. Ridley, and W. J. Schaff, Semicond. Sci. Technol. **19**, 427 (2004).
[15]M. N. Gurusinghe, S. K. Davidsson, and T. G. Andersson, Phys. Rev. B **72**, 045316 (2005).
[16]J. S. Speck and S. J. Rosner, Phys. B **273–274**, 24 (1999).
[17]D. N. Quang, N. H. Tung, and N. T. Tien, J. Appl. Phys. **109**, 113711 (2011).
[18]L. Hsu and W. Walukiewicz, J. Appl. Phys. **89**, 1783 (2001).
[19]S. Keller, G. Parish, P. T. Fini, S. Heikman, C.-H. Chen, N. Zhang, S. P. DenBaars, U. K. Mishra, and Y.-F. Wu, J. Appl. Phys. **86**, 5850 (1999).
[20]S. Arulkumaran, T. Egawa, H. Shikawa, and T. Jimbo, J. Vac. Sci. Tecnol. B **21**, 888 (2003).
[21]M. Miyoshi, T. Egawa, and H. Shikawa, J. Vac. Sci. Tecnol. B **23**, 1527 (2005).
[22]K. Köhler, S. Müller, P. Waltereit, W. Pletschen, V. Polyakov, T. Lim, L. Kirste, H. P. Menner, P. Brückner, O. Ambacher, C. Buchleim, and R. Goldhahn, J. Appl. Phys. **109**, 053705 (2011).
[23]L. Hsu and W. Walukiewicz, Phys. Rev. B **56**, 1520 (1997).
[24]J. Antoszewski, M. Gracey, J. M. Dell, L. Faraone, T. A. Fisher, G. Parish, Y.-F. Wu, and U. K. Mishra, J. Appl. Phys. **87**, 3900 (2000).
[25]A. Gold and W. Götze, J. Phys. C **14**, 4049 (1981); Phys. Rev. B **33**, 2495 (1986).
[26]F. Stern and W. E. Howard, Phys. Rev. **163**, 816 (1967).
[27]A. Gold, Phys. Rev. B **35**, 723 (1987).
[28]Y. Okuyama and N. Tokuda, Phys. Rev. B **40**, 9744 (1989).
[29]T. Ando, J. Phys. Soc. Jpn. **51**, 3893 (1982); **51**, 3900 (1982).
[30]N. T. Tien, D. N. Thao, P. T. B. Thao, and D. N. Quang, Phys. B **479**, 62 (2015).
[31]M. Jonson, J. Phys. C **9**, 3055 (1976).
[32]G. Bastard, *Wave Mechanics Applied to Semiconductor Heterostructures* (Les Editions de Physique, Paris, 1988).
[33]O. Ambacher, B. Foutz, J. Smart, J. R. Shealy, N. G. Weimann, K. Chu, M. Murphy, A. J. Sierakowski, W. J. Shaff, L. F. Eastman, R. Dimitrov, A. Mitchell, and M. Stutzmann, J. Appl. Phys. **87**, 334 (2000).
[34]N. Maeda, T. Nishida, N. Kobayashi, and M. Tomizawa, Appl. Phys. Lett. **73**, 1856 (1998).
[35]T.-H. Yu and K. F. Brennan, J. Appl. Phys. **89**, 3827 (2001).
[36]D. Jena, S. Heikman, J. S. Speck, A. Gossard, and U. Mishra, Phys. Rev. B **67**, 153306 (2003).
[37]D. Jena, Y. P. Smorchkova, C. R. Elsass, A. C. Gossard, and U. K. Mishra, in *Proceedings of the 25th International Conference on Physics of Semiconductors*, edited by N. Miura and T. Ando (Osaka, 2000), p. 771.
[38]T. Ando, J. Phys. Soc. Jpn. **43**, 1616 (1977).
[39]Y. Matsumoto and Y. Uemura, Jpn. J. Appl. Phys., Suppl. 2, Pt. 2, 367 (1974).
[40]F. F. Fang and W. E. Howard, Phys. Rev. Lett. **16**, 797 (1966).
[41]F. Bernardini, V. Fiorentini, and D. Vanderbilt, Phys. Rev. B **56**, R10024 (1997).
[42]I. P. Smorchkova, C. R. Elsass, J. P. Ibbetson, R. Vetury, B. Heying, P. Fini, E. Haus, S. DenBaars, J. S. Spect, and U. K. Mishra, J. Appl. Phys. **86**, 4520 (1999).
[43]I. P. Smorchkova, L. Chen, T. Mates, L. Shen, S. Heikman, B. Moran, S. Keller, S. P. DenBaars, J. P. Speck, and U. K. Mishra, J. Appl. Phys. **90**, 5196 (2001).